Journal of Fluorine Chemistry 144 (2012) 51–58

Contents lists available at SciVerse ScienceDirect

Journal of Fluorine Chemistry

journal homepage: www.elsevier.com/locate/fluor

Buckminsterfullerene derivatives bearing a fluoroalkyl group for use in organic photovoltaic cells

Makoto Karakawa [a], Takabumi Nagai [b], Tomomi Irita [b], Kenji Adachi [b], Yutaka Ie [a], Yoshio Aso [a,*]

[a] Department of Soft Nanomaterials, Nanoscience and Nanotechnology Center, The Institute of Scientific and Industrial Research (ISIR), Osaka University, 8-1 Mihogaoka, Ibaraki, Osaka 567-0047, Japan
[b] Fundamental Technology Group, Chemical R&D Center, Daikin Industries, Ltd., 1-1 Nishi Hitotsuya, Settsu, Osaka 566-8585, Japan

ARTICLE INFO

Article history:
Received 2 July 2012
Received in revised form 25 September 2012
Accepted 25 September 2012
Available online 3 October 2012

Keywords:
Fullerene derivative
Perfluoroalkyl
n-Type semiconductor
Photovoltaic cell

ABSTRACT

Six novel fluoroalkylpyrrolidine-substituted [60]fullerene derivatives were synthesized and their ability to perform as new n-type organic photovoltaic materials was evaluated. The fullerene derivatives were soluble in common organic solvents, affording good processability properties for the fabrication of photovoltaic cells, and showed an absorption range and molar extinctions similar to those of [6,6]-phenyl C_{61} butyric acid methyl ester. Bulk-heterojunction photovoltaic cells using poly(3-hexylthiophene):fullerene derivative blends as the photovoltaic active layers were fabricated and characterized. The performances of the photovoltaic cells were notably affected by the substituents on the fullerene derivatives. Short fluoroalkyl (C_4F_9) chains on pyrrolidine-linked phenyl groups were suitable substituents for the photovoltaic materials in the current study. This fullerene derivative bearing a C_4F_9-phenyl group showed a moderate power conversion efficiency of 0.53% during simulated AM 1.5 G solar irradiation at 100 mW/cm^2. This is so far the first report of the use of fluoroalkyl fullerene derivatives as the active materials in organic photovoltaic cells.

1. Introduction

Organic photovoltaic (OPV) cells based on conjugated polymers and soluble fullerene derivatives have attracted a great deal of attention because of their solution processability and mechanical flexibility properties and their potential low-cost large-module fabrication [1–14]. The soluble buckminsterfullerene derivative, [6,6]-phenyl C_{61} butyric acid methyl ester ($PC_{61}BM$), is currently the most promising acceptor material for OPV cells. The power conversion efficiency (PCE) of poly(3-hexylthiophene) (P3HT)/$PC_{61}BM$ bulk-heterojunction (BHJ) solar cells has been improved up to 6% under specially optimized conditions [1–5].

To make further progress in OPV materials and physics, developing a deeper understanding of the compatibility, miscibility, and dispersibility in OPV materials is necessary to allow for the fabrication of an ideal p–n juncture between a donor and an acceptor material in a blend film. We cannot, however, select an alternative acceptor material to $PC_{61}BM$ for OPV fabrication at present. This lack of alternative acceptor materials has led to an overall lack of fundamental understanding and has severely limited the development of any further improvement in OPV performance. In light of these limitations, several new fullerene derivatives have been developed in recent years [15–21]. Cao et al. [15] reported the synthesis of methanofullerenes containing several long-alkyl ester groups from $PC_{61}BM$. They subsequently concluded that the synthesis of an acceptor that has good compatibility with donor polymer materials is important for improving device performance. Blom et al. [16] reported that fullerene bis-adducts with higher LUMO levels effectively enhanced the open-circuit voltage and PCE values to a greater extent than that of the corresponding fullerene mono-adducts. In 2008, Wudl et al. [17] developed functionalized methanofullerenes based on the $PC_{61}BM$ with a branched alkoxy side chain on a phenyl group. These compounds provided PCE values of 1.73% from a standard photovoltaic cell. The efficiency was further improved up to 2.64% when a TiOx layer was introduced as a spacer between the active layer and the Al cathode. In a separate development in 2009, Wudl et al. [18] reported an isomeric iminofullerene and its positive effect in enhancing short-circuit currents. In a more detailed study, two other groups [19–21] investigated the relationship between material structure and photovoltaic performance, and the studies revealed that the solubility of the fullerene derivatives and their intermolecular interactions had an impact on the OPV cell parameters. These reports have provided us with some important information about the relationship between the chemical structures of the materials and the device characteristics. The suitably modified chemical structures of the materials can induce not only the function of high carrier mobility but also the

* Corresponding author. Tel.: +81 6 6879 8476; fax: +81 6 6879 8479.
E-mail address: aso@sanken.osaka-u.ac.jp (Y. Aso).

0022-1139/$ – see front matter © 2012 Elsevier B.V. All rights reserved.
http://dx.doi.org/10.1016/j.jfluchem.2012.09.009

compatibility in the blend film, which are important characteristics of the materials.

Chikamatsu et al. developed long-chain perfluoroalkyl-substituted C_{60} derivatives and investigated their field-effect transistor (FET) properties. They demonstrated a field-effect mobility of the order of 10^{-1} cm^2/V s as well as the device-operation air stability of the compounds [22,23]. We believed that high performance materials for n-channel FETs such as perfluoroalkyl substituted C_{60} derivatives could be potential candidates for acceptor materials in the next generation of OPV cells. The characteristic nature of the perfluoroalkyl group, however, must be considered. For instance, Hashimoto et al. reported the attempted use of a fullerene derivative with a fluoroalkyl chain (F-$PC_{61}BM$) in an OPV cell. The F-$PC_{61}BM$ did not work as the active material of the BHJ type device, but was used as an additive to form a self-organized buffer layer, improving the fill factor of the device as a consequence of its strong phase separation ability [24]. As stated above, there are no reported examples of the use of fullerene derivatives containing fluoroalkyl groups as the active acceptor materials in OPV cell.

In the current paper, we report the synthesis of several new fullerene derivatives containing fluoroalkyl groups of different lengths, together with their photophysical, electrochemical, and photovoltaic properties. Our study of the BHJ OPV cell using P3HT:fullerene-derivative blend film as the active layer provided a PCE value up to 0.53% under simulated AM 1.5 G solar irradiation at 100 mW/cm^2. This represents so far the first demonstration of the successful use of a fluoroalkyl fullerene derivative as the active material in organic photovoltaic cells.

2. Experimental

2.1. Materials

Reagents were purchased from Wako Pure Chemical Industries, Tokyo Kasei Chemical Industries, Merck Ltd., and Aldrich, and used without further purification. [60]Fullerene was purchased from Honjo Chemical Corporation. Compounds **1**, **8**, **9** (Scheme 1), amino acid derivatives [2-(methylamino)decanoic acid, *N*-dodecylglycine, and 2-(dodecylamine)hexadecanoic acid], and perfluroalkylbenzaldehyde derivatives (4-heptadecafluorooctylbenzaldehyde, 4-tridecafluorohexylbenzaldehyde, and 4-nonafluorobenzaldehyde) were synthesized according to the literature [25–30]. Compound **10** was purchased from Aldrich.

2.2. Apparatus

UV–vis absorption spectra were recorded on Shimadzu UV-3100PC. All spectra were obtained in spectrograde solvents. ^1H and ^{19}F NMR were recorded with JEOL JNM-ECS400 (400 MHz) and ^{13}C NMR spectra were recorded with a Bruker BioSpin AVANCE III 700 (700 MHz) spectrometer in chloroform-*d* [chemical shifts in parts per million (ppm) downfield from tetramethylsilane as an internal standard for ^1H and ^{13}C and upfield from fluorotrichloromethane as an internal standard for ^{19}F]. Cyclic voltammetry was carried out on a BAS CV-50W voltammetric analyzer using a Pt electrode in a 0.1 mol/L Bu_4NPF_6 in chlorobenzene/CH_3CN (5:1, v/v) solution. The synthesized fullerene derivatives were purified by a recycling mode of preparative gel-permeation liquid chromatography (GPLC) with the use of Jasco LC-9201S equipped with a refractive index detector using JAIGEL 1H/2H columns and Japan Analytical Industry LC-908 equipped with JAIGEL 1H/2H columns (eluent: $CHCl_3$). The HPLC measurements were carried out by gel permeation chromatography in chloroform at 40 °C. Hitachi UV/vis detector (L-2400), Hitachi pump (L-2130), TOSOH GPC system (GPC-8200 model II ver. 6.0), and Shodex column (GPC K-803L and GPC K-G Guard Column) were used. The flow rate was 1.0 mL/min. Column chromatography was performed on silica gel, KANTO Chemical silica gel 60N (40–50 μm). Elemental analyses were performed on Perkin Elmer LS-50B by the Elemental Analysis Section of Comprehensive Analysis Center (CAC) of ISIR, Osaka University. The thicknesses of the thin films were measured using a HORIBA Jobin Yvon UVISEL LT NIR-NNG spectroscopic ellipsometer. The surface morphology of the deposited organic film was observed using an atomic force microscope (Shimadzu, SPM9600). X-ray diffraction measurements of the organic films were carried out on Rigaku Ultima IV using Cu *Kα* radiation (40 kV, 40 mA) with a curved graphite monochromator. The diffractions were measured from 3° to 30° in the 2θ–θ scan mode with a 0.01° step.

2.3. Device fabrication and measurements

Glass slides patterned with ITO (Sanyo Vacuum Industries Co., Ltd.) were treated in an O_2 plasma oven for 5 min. Thereafter, the

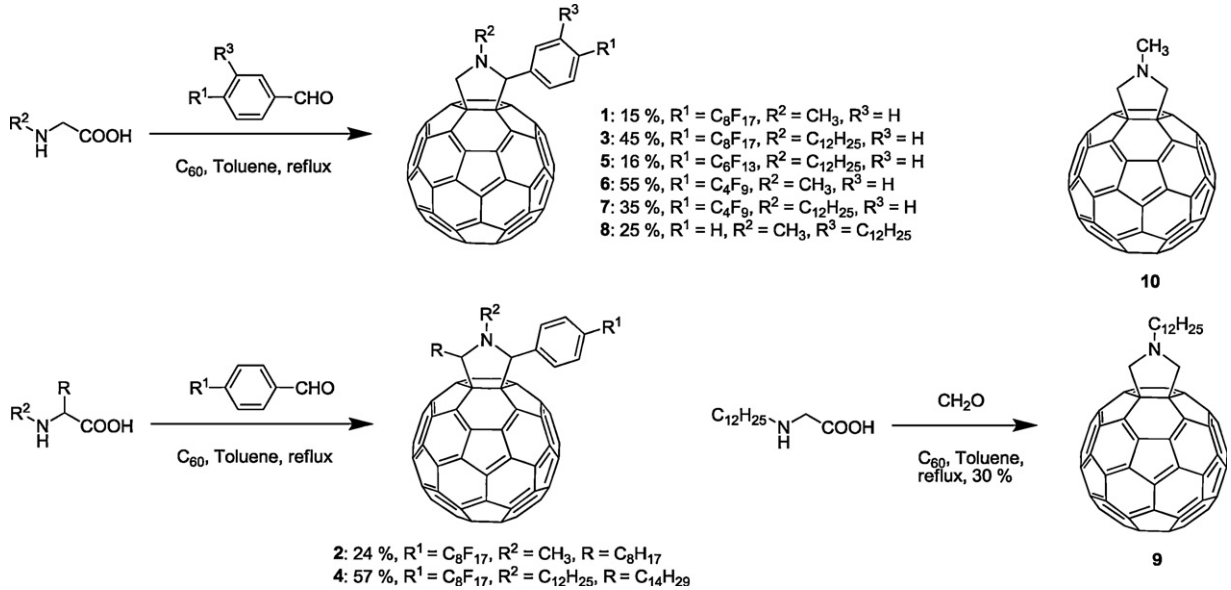

Scheme 1. Synthetic route to the fullerene derivatives, **1**–**9**, and the structure of compound **10**.

ITO-coated grass slides were spin-coated (500 rpm for 5 s and 3000 rpm for 60 s) with a filtered (0.45 μm pore size PTFE membrane filter) aqueous suspension of poly(ethylene dioxythiophene) doped with poly(styrenesulfonic acid) (PEDOT-PSS) (Clevios P VP Al 4083), and then baked at 135 °C for 10 min in air. P3HT (Merck Ltd.) and a fullerene derivative (1:1 or 2:1, wt/wt) were dissolved in chloroform at room temperature and then spun-cast on the top of the PEDOT-PSS layer at 1500 rpm for 60 s. The thicknesses of the resulting P3HT/fullerene-derivative films were found to be ca. 180 nm, which were confirmed by ellipsometry measurements. The device fabrication was completed by the vacuum deposition of Al cathode (ca. 800 nm). The active area of each solar cell device was 3 mm × 3 mm. The solar cells were subsequently tested under simulated air mass (AM) 1.5 G solar irradiation (100 mW/cm^2, SAN-EI ELECTRIC CO., LTD. XES-301S). Current–voltage (*J*–*V*) characteristics were recorded using a PC-controlled Keithley 2400 source meter.

2.4. Synthesis

2.4.1. Typical procedure for the synthesis of fulleropyrrolidine derivative

A mixture of amino acid (4.0 mmol), benzaldehyde (1.0 mmol), and C_{60} (2.0 mmol) was refluxed in toluene (300 mL) under a N_2 atmosphere for 20–64 h. After vacuum evaporation of the solvent, the crude product was purified by preparative GPLC using chloroform as eluent to give the desired product.

2.4.2. C_{60}-fused N-methyl-5-octyl-2-(4-heptadecafluorooctyl)phenylpyrrolidine (**2**)

2 was synthesized according to the typical procedure; Yield 24.0%; ^{1}H NMR (400 MHz, $CDCl_3$): 0.87 (t, *J* = 8.0 Hz, 3H), 1.18–1.67 (m, 10H), 1.67–1.93 (m, 2H), 2.50–2.64 (m, 1H), 2.50–2.64 (m, 1H), 2.86 (s, 3H), 4.91 (d-d, *J* = 8.1, 2.4 Hz, 1H), 5.58 (s, 1H), 7.62 (d, *J* = 8.0 Hz, 2H), 7.90 (d, *J* = 8.0 Hz, 2H); ^{19}F NMR (372 MHz, $CDCl_3$, *δ*): −80.65 (t, *J* = 9.8 Hz, 3F), −110.58 (t, *J* = 13.1 Hz, 2F), −120.90 to −121.20 (m, 2F), −121.55 to −121.95 (m, 4F), −121.95 to −122.15 (m, 2F), −122.44 to −122.74 (m, 2F), −125.88 to −126.10 (m, 2F); ^{13}C NMR (175 MHz, $CDCl_3$, *δ*): 14.14, 22.71, 26.25, 29.00, 29.22, 29.38, 29.94, 31.86, 35.29, 73.78, 75.38, 106–120.5 (m, C_8F_{17}), 126.84 (bs), 128.85 (t, J_{C-C-F} = 23.5 Hz), 129.99 (bs), 135.79, 136.47, 136.75, 139.33, 139.58, 141.51, 141.59, 141.78, 141.82, 141.94, 141.97, 142.08, 142.12, 142.15, 142.17, 142.28, 142.47, 142.57, 142.63, 142.65, 142.81, 143.11, 143.20, 144.37, 144.50, 144.60, 144.67, 145.19, 145.20, 145.28, 145.38, 145.41, 145.44, 145.45, 145.49, 145.66, 145.69, 146.00, 146.03, 146.15, 146.17, 146.28, 146.31, 146.33, 146.50, 146.79, 147.35, 147.37, 152.76, 153.59, 157.15; UV–vis ($CHCl_3$): λ_{max} (*ε*) = 256 nm (105,000); Anal. calcd for $C_{85}H_{26}NF_{17}$: C 73.76, H 1.89, N 1.01; Found: C 73.49, H 2.11, N 1.06.

2.4.3. C_{60}-fused N-dodecyl-2-(4-heptadecafluorooctyl)phenylpyrrolidine (**3**)

3 was synthesized according to the typical procedure; Yield 45.6%; ^{1}H NMR (400 MHz, $CDCl_3$, *δ*): 0.89 (t, *J* = 8.0 Hz, 3H), 1.20–1.75 (m, 18H), 1.80–2.06 (m, 2H), 2.52–2.66 (m, 1H), 3.10–3.26 (m, 1H), 4.16 (d, *J* = 9.0 Hz, 1H), 5.13 (d, *J* = 9.0 Hz, 1H), 5.14 (s, 1H), 7.64 (d, *J* = 8.0 Hz, 2H), 7.98 (bs, 2H); ^{19}F NMR (372 MHz, $CDCl_3$, *δ*): −80.57 (t, *J* = 9.8 Hz, 3F), −110.55 (t, *J* = 13.7 Hz, 2F), −120.90 to −121.20 (m, 2F), −121.50 to −122.10 (m, 6F), −122.44 to −122.70 (m, 2F), −125.85 to −126.05 (m, 2F); ^{13}C NMR (175 MHz, $CDCl_3$, *δ*): 14.12, 22.71, 27.51, 28.33, 29.39, 29.68, 29.70, 29.74, 31.96, 53.28, 66.92, 68.98, 76.39, 81.93, 106–120.5 (m, C_8F_{17}), 127.08 (bs), 128.94 (t, J_{C-C-F} = 24.1 Hz), 129.80 (bs), 135.61, 136.00, 136.50, 136.96, 139.44, 139.94, 140.24, 140.26, 141.53, 141.72, 141.86, 141.87, 141.98, 142.06, 142.11, 142.17, 142.18, 142.28, 142.34, 142.59, 142.63, 142.64, 142.75, 143.05, 143.20, 144.40, 144.46, 144.61, 144.76, 145.23, 145.27, 145.32, 145.39, 145.49, 145.54, 145.57, 145.59, 145.68, 145.71, 145.99, 146.00, 146.16, 146.20, 146.23, 146.26, 146.32, 146.37, 146.38, 146.47, 147.38, 152.67, 152.94, 154.05, 156.26; UV–vis ($CHCl_3$): λ_{max} (*ε*) = 256 nm (114,000); Anal. calcd for $C_{88}H_{32}NF_{17}$: C 74.11, H 2.26, N 0.98; Found: C 74.04, H 2.35, N 1.00.

2.4.4. C_{60}-fused N-dodecyl-5-tetradecyl-2-(4-heptadecafluorooctyl)phenylpyrrolidine (**4**)

4 was synthesized according to the typical procedure; Yield 56.9%; ^{1}H NMR (400 MHz, $CDCl_3$, *δ*): 0.80–1.00 (m, 6H), 1.00–2.05 (m, 44H), 2.41–2.60 (m, 1H), 2.60–2.75 (m, 1H), 2.90–3.05 (m, 1H), 3.05–3.20 (m, 1H), 4.96 (d, *J* = 8.0 Hz, 1H), 5.63 (s, 1H), 7.60 (d, *J* = 8.0 Hz, 2H), 7.88 (d, *J* = 8.0 Hz, 2H); ^{19}F NMR (372 MHz, $CDCl_3$, *δ*): −80.59 (t, *J* = 10.0 Hz, 3F), −110.53 (t, *J* = 12.2 Hz, 2F), −120.86 to −121.20 (m, 2F), −121.46 to −122.10 (m, 6F), −122.42 to −122.72 (m, 2F), −125.85 to −126.06 (m, 2F); ^{13}C NMR (175 MHz, $CDCl_3$, *δ*): 14.22, 14.24, 22.82, 25.00, 27.53, 28.29, 28.92, 29.45, 29.51, 29.62, 29.79, 29.82, 29.84, 29.88, 30.02, 32.06, 46.32, 70.65, 73.59, 76.55, 76.71, 106–120 (m, C_8F_{17}), 126.83 (bs), 128.78 (t, J_{C-C-F} = 24.3 Hz), 130.14 (bs), 135.93, 136.48, 136.90, 136.96, 139.30, 139.60, 140.06, 140.27, 141.56, 141.64, 141.88, 142.01, 142.03, 142.20, 142.25, 142.33, 142.35, 142.63, 142.66, 142.71, 142.88, 143.16, 143.26, 144.44, 144.59, 144.70, 144.74, 145.23, 145.25, 145.31, 145.34, 145.45, 145.48, 145.55, 145.61, 145.73, 145.76, 146.06, 146.08, 146.22, 146.24, 146.35, 146.37, 146.38, 146.40, 146.63, 146.99, 147.41, 147.43, 152.89, 153.64, 153.91, 157.46; UV–vis ($CHCl_3$): λ_{max} (*ε*) = 256 nm (106,000); Anal. calcd for $C_{102}H_{60}NF_{17}$: C 75.50, H 3.73, N 0.86; Found: C 75.33, H 3.74, N 0.95.

2.4.5. C_{60}-fused N-dodecyl-2-(4-tridecafluorohexyl)phenylpyrrolidine (**5**)

5 was synthesized according to the typical procedure; Yield 16.8%; ^{1}H NMR (400 MHz, $CDCl_3$, *δ*): 0.89 (t, *J* = 6.8 Hz, 3H), 1.20–1.60 (17 H, m), 1.60–1.75 (m, 1H), 1.82–2.05 (m, 2H), 2.50–2.62 (m, 1H), 3.12–3.23 (m, 1H), 4.15 (d, *J* = 9.6 Hz, 1H), 5.12 (d, *J* = 9.6 Hz, 1H), 5.13 (s, 1H), 7.63 (d, *J* = 8.7 Hz, 2H), 7.97 (bs, 2H); ^{19}F NMR (372 MHz, $CDCl_3$, *δ*): −80.66 (t, *J* = 9.9 Hz, 3F), −110.56 (t, *J* = 13.7 Hz, 2F), −121.10 to −121.40 (m, 2F), −121.90 to −122.10 (m, 2F), −122.60 to −122.80 (m, 2F), −125.80 to −126.10 (m, 2F); ^{13}C NMR (175 MHz, $CDCl_3$, *δ*): 14.13, 22.70, 27.50, 28.33, 29.39, 29.67, 29.70, 29.74, 31.94, 53.27, 66.86, 68.92, 76.33, 81.85, 106–120.5 (m, C_6F_{13}), 127.06 (bs), 128.84 (t, J_{C-C-F} = 24.2 Hz), 129.62 (bs), 135.59, 135.98, 136.41, 136.92, 141.50, 141.67, 141.82, 141.95, 142.01, 142.03, 142.06, 142.07, 142.12, 142.14, 142.24, 142.30, 142.56, 142.58, 142.59, 142.70, 143.01, 143.15, 144.36, 144.42, 144.56, 144.71, 145.18, 145.22, 145, 27, 145.35, 145.45, 145.49, 145.54, 145.55, 145.63, 145.67, 145.94, 145.96, 146.11, 146.15, 146.19, 146.22, 146.28, 146.31, 146.34, 146.42, 152.62, 152.87, 153.99, 156.21; UV–vis ($CHCl_3$): λ_{max} (*ε*) = 256 nm (93,000); Anal. calcd for $C_{86}H_{32}NF_{13}$: C 77.89, H 2.43, N 1.06; Found: C 77.69, H 2.65, N 1.05.

2.4.6. C_{60}-fused N-methyl-2-(4-nonafluorobutyl)phenylpyrrolidine (**6**)

6 was synthesized according to the typical procedure; Yield 55.5%; ^{1}H NMR (400 MHz, $CDCl_3$, *δ*): 2.82 (s, 3H), 4.30 (d, *J* = 9.6 Hz, 1H), 5.01 (d, *J* = 9.6 Hz, 1H), 5.01 (s, 1H), 7.66 (d, *J* = 8.2 Hz, 2H), 7.97 (bs, 2H); ^{19}F NMR (372 MHz, $CDCl_3$, *δ*): −80.85 (3F, t-t, *J* = 9.3, 2.7 Hz), −110.78 (t, *J* = 13.1 Hz, 2F), −122.59 to −122.79 (m, 2F), −125.36 to −125.53 (m, 2F); ^{13}C NMR (175 MHz, $CDCl_3$, *δ*): 40.03, 70.07, 82.92, 106–120 (m, C_4F_9), 127.18 (bs), 128.94 (t, J_{C-C-F} = 24.2 Hz), 129.78 (bs), 135.65, 136.04, 136.38, 136.98, 139.51, 139.97, 140.27, 141.58, 141.74, 141.88, 141.90, 142.01, 142.04,

142.11, 142.20, 142.26, 142.28, 142.60, 142.64, 142.65, 142.76, 143.06, 143.20, 144.39, 144.75, 145.25, 145.33, 145.36, 145.41, 145.54, 145.60, 145.68, 145.72, 146.00, 146.02, 146.17, 146.21, 146.27, 146.35, 147.37, 147.38, 152.49, 152.80, 153.79, 155.94; UV–vis ($CHCl_3$): λ_{max} (ε) = 256 nm (116,000); Anal. calcd for $C_{73}H_{10}NF_9$: C 81.80, H 0.94, N 1.31; Found: C 81.58, H 1.22, N 1.31.

2.4.7. C_{60}-fused N-dodecyl-2-(4-nonafluorobutyl)phenylpyrrolidine (**7**)

7 was synthesized according to the typical procedure; Yield 35.3%; ^{1}H NMR (400 MHz, $CDCl_3$, δ): 0.88 (t, J = 7.0 Hz, 3H), 1.10–1.60 (m, 17H), 1.60–1.75 (m, 1H), 1.80–2.05 (m, 2H), 2.55–2.65 (m, 1H), 3.10–3.25 (m, 1H), 4.15 (d, J = 10.2 Hz, 1H), 5.12 (d, J = 10.2 Hz, 1H), 5.13 (s, 1H), 7.64 (d, J = 9.0 Hz, 2H), 7.97 (bs, 2H); ^{19}F NMR (372 MHz, $CDCl_3$, δ): −80.85 (t-t, J = 9.3, 2.9 Hz, 3F), −110.76 (t, J = 12.6 Hz, 2F), −122.61 to −122.78 (m, 2F), −125.35 to −125.52 (m, 2F); ^{13}C NMR (175 MHz, $CDCl_3$, δ): 14.13, 22.71, 27.51, 28.32, 29.39, 29.68, 29.70, 29.74, 31.96, 53.27, 66.92, 68.98, 76.38, 81.95, 106–120 (m, C_4F_9), 127.08 (bs), 128.84 (t, J_{C-C-F} = 24.5 Hz), 129.76 (bs), 135.69, 136.00, 136.44, 136.98, 139.44, 140.25, 140.27, 141.56, 141.72, 141.87, 142.01, 142.06, 142.10, 142.11, 142.17, 142.18, 142.29, 142.59, 142.63, 142.64, 142.75, 143.05, 143.20, 144.40, 144.46, 145.23, 145.27, 145.31, 145.33, 145.39, 145.40, 145.49, 145.54, 145.57, 145.59, 145.71, 145.99, 146.01, 146.20, 146.32, 146.37, 146.48, 147.38, 152.67, 152.94, 154.05, 156.26; UV–vis ($CHCl_3$): λ_{max} (ε) = 256 nm (109,000); Anal. calcd for $C_{84}H_{32}NF_9$: C 82.28, H 2.63, N 1.14; Found: C 82.09, H 2.91, N 1.20.

3. Results and discussion

3.1. Synthesis of fluoroalkyl [60]fullerene derivatives

The motivation for the design and synthesis of these fullerene derivatives was to look for novel fullerene derivatives for application as the acceptors in next generation OPV materials. We were also keen to investigate the effect that incorporating fluoroalkyl chains in fullerene derivatives have on the photovoltaic properties. Our strategy for developing novel fullerene derivatives with high carrier mobility involved the introduction of a fluoroalkyl group onto the fullerene framework through a pyrrolidine ring. It was envisaged that the fluoroalkyl group would enhance the aggregation properties of the fullerene derivatives and provide better intermolecular interactions. With all of this in mind, a series of fulleropyrrolidine derivatives with a *p*-perfluoroalkylphenyl group **1**–**7** were designed and synthesized. The synthetic methodology is depicted in Scheme 1. Alkylated amino acids [25–27] and *p*-perfluoroalkylbenzaldehyde [28] derivatives are two key starting materials, which were prepared according to standard synthetic procedures from the corresponding amino acid and *p*-iodobenzaldehyde derivatives, respectively. [60]Fullerene was treated under the Prato reaction conditions [29,30] with the *N*-alkylated amino acids and the corresponding *p*-perfluoroalkylbenzaldehyde derivatives. The reactions proceeded smoothly and afforded moderate yields of the corresponding fulleropyrrolidene derivatives, which were purified by preparative GPLC using chloroform as eluent to remove any byproducts. Non-fluorinated alkyl derivatives **8** and **9** were similarly prepared as reference compounds. The desired products were obtained as black or brown powders and were fully characterized with ^{1}H, ^{19}F, and ^{13}C NMR spectroscopy, elemental analysis and HPLC measurements (the HPLC chart are shown in the supplementary material). *N*-Methylfulleropyrrolidine (**10**) was purchased from Aldrich. All of the fulleropyrrolidine derivatives except compound **10** dissolve well in chlorinated organic solvents, such as chloroform, chlorobenzene, and *o*-dichlorobenzene, providing good processability properties for OPV cell fabrication.

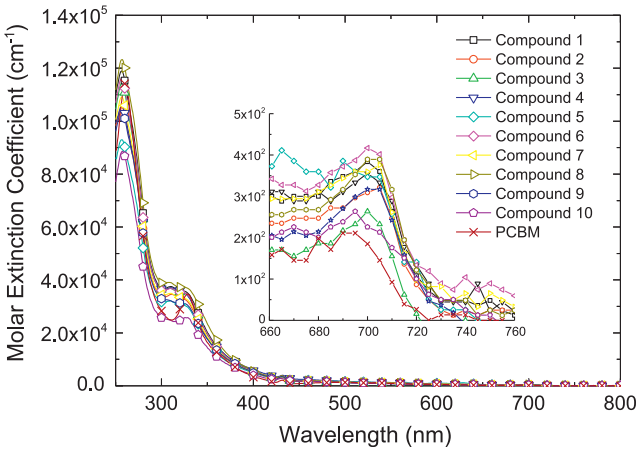

Fig. 1. UV–vis absorption spectra of the fullerene derivatives, **1**–**10** and $PC_{61}BM$ in a $CHCl_3$ solution.

3.2. Electronic absorption properties

The UV–vis absorption spectra of the fullerene derivatives **1**–**10** together with the spectrum of $PC_{61}BM$ in chloroform are shown in Fig. 1. All the compounds showed an absorption band in the range of 250–350 nm and the peak maximum was observed at 260 nm. Weak absorption peaks were also detected in all of the compounds around 700 nm, which correspond to the π–π^* transition of the fullerene framework. It is clear from the spectra that the substituent groups on the fullerenes do not affect the electronic structure of the fullerene π system because the spectra were all very similar in shape and showed similar molar extinction coefficients.

3.3. Electrochemical properties

To investigate the electrochemical properties of the fullerene derivatives and estimate their LUMO energy levels, cyclic voltammetry (CV) measurements were conducted in a 5:1 (v/v) mixture of chlorobenzene:CH_3CN. The LUMO energy levels (E_{LUMO}s) of the compounds were estimated using the following empirical equation: $E_{LUMO} = E^1_{1/2} + 4.8$ eV, where $E^1_{1/2}$ is the value of first reduction potential relative to that of ferrocene/ferrocenium (Fc/Fc^+) [31]. Representative examples of the resulting CV curves are shown in Fig. 2, and the numerical data of all the compounds are summarized in Table 1 (the remaining CV curves are shown in the supplementary material). For the sake of comparison, the CV curve and associated data from $PC_{61}BM$ are also shown in Fig. 2 and Table 1, respectively. All the fullerene derivatives underwent reversible reduction processes and the CV curves were unchanged following successive multiple potential scans, indicating the high stability of the materials for electron injection. It is clear from the CV curves and associated data that all of the fullerene derivatives exhibited reduction potential values similar to that of $PC_{61}BM$. Thus the LUMO energy levels of all of the derivatives are in the range of −3.6 to −3.7 eV. Although the compounds contain the strong-electron-withdrawing perfluoroalkyl chains, these substituents do not affect the frontier-orbital energy levels of the compounds.

3.4. Photovoltaic properties

The OPV properties of the fluoroalkyl as well as non-fluoroalkyl fullerene derivatives were investigated using BHJ OPV cells with a device structure of ITO/PEDOT-PSS/P3HT:fullerene derivative/Al, where the polymer P3HT was used as the electron donor and the

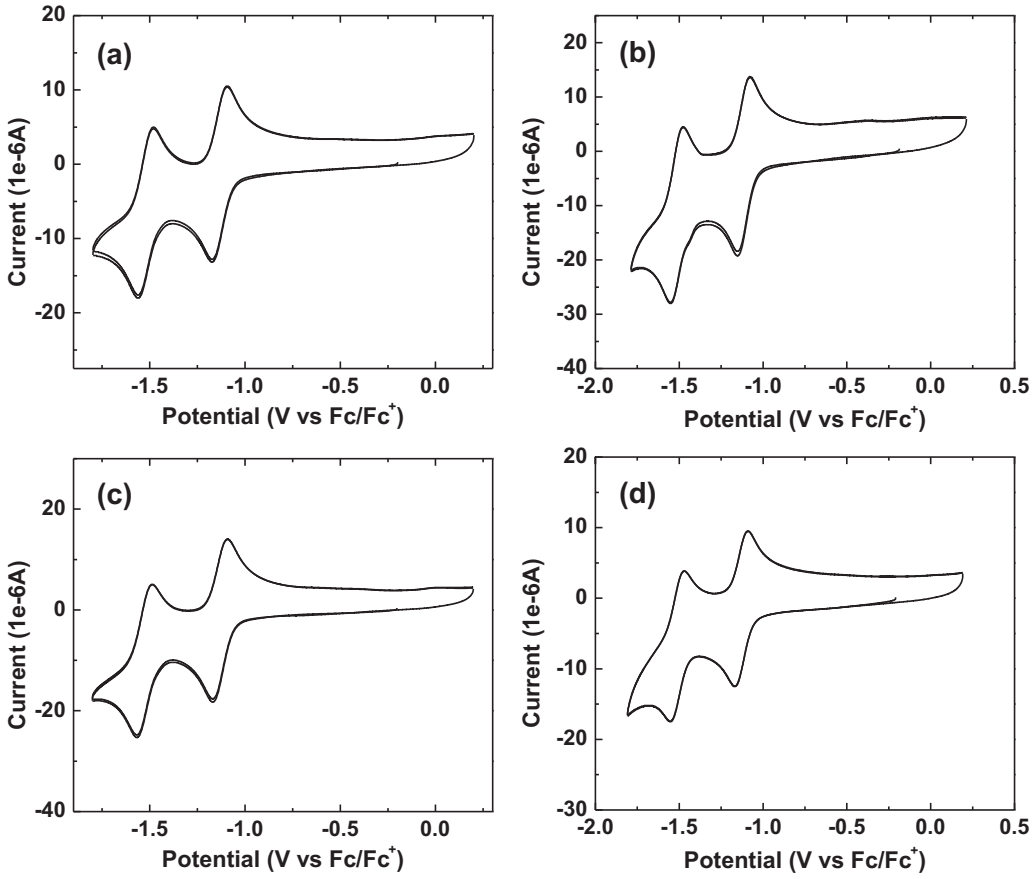

Fig. 2. Cyclic voltammograms of the fullerene derivatives: (a) compound **3**, (b) compound **5**, (c) compound **7**, and (d) $PC_{61}BM$, in a chlorobenzene/CH_3CN (5:1, v/v) solution.

fullerene derivatives were used as the electron acceptors. The active layer was fabricated by spin-cast from a chloroform solution as opposed to a chlorobenzene solution because the slow evaporation of the chlorobenzene solvent induced the unfavorable aggregation of the fluoroalkyl fullerene derivatives owing to the strong intermolecular interactions between the fluoroalkyl groups. For the sake of comparison on the same conditions, OPV cells using fullerene derivatives without fluoroalkyl group were also fabricated according to the same procedures.

The current density–voltage (*J*–*V*) characteristics of the OPV cells fabricated from compounds **3**, **5**, **6**, and **7** in the absence of light and under simulated AM 1.5 G solar irradiation at 100 mW/cm^2 are shown in Fig. 3. The OPV cell based on P3HT:$PC_{61}BM$ was also fabricated and measured as a reference cell (the *J*–*V* curve of the cell is shown in the supplementary material). The performance data of the OPV cells, including open-circuit voltage (V_{oc}), short-circuit current density (J_{sc}), fill factor (FF), and PCE values are summarized in Table 2 for a clear comparison.

Table 1
Reduction potentials and LUMO energy levels of the fullerene derivatives.

Compound	$E^1_{1/2}$ (V vs Fe/Fe$^+$)	$E^2_{1/2}$ (V vs Fe/Fe$^+$)	LUMO (eV)[a]
1	−1.13	−1.52	−3.67
2	−1.14	−1.53	−3.66
3	−1.14	−1.52	−3.66
4	−1.17	−1.55	−3.63
5	−1.17	−1.54	−3.63
6	−1.11	−1.51	−3.69
7	−1.11	−1.51	−3.69
8	−1.13	−1.52	−3.67
9	−1.16	−1.55	−3.64
10	−1.14	−1.53	−3.66
$PC_{61}BM$	−1.13	−1.51	−3.67

[a] The values were estimated from the first reduction potentials of the compounds.

The OPV cells containing long fluoroalkyl (C_8F_{17}) fullerene derivatives as the acceptors showed significantly lower PCE values of less than 0.14%. Furthermore, in spite of their good performance from the perspective of the n-type field-effect transistor properties of the compounds [32], the cells experienced a high series resistance leading to lower FF and J_{sc} values. Relative to these long fluoroalkyl fullerene derivatives, the PCE values of compounds **2** and **4** were half those of compounds **1** and **3**. These differences could be attributed to the chemical structures of compounds **2** and **4**, which contain a long alkyl group at the *C*-5 position of the pyrrolidine ring, whereas compounds **1** and **3** possess no alkyl group at the same position. This led us to the formulation of a tentative theory, which suggested that steric hindrance derived from the long alkyl group at the *C*-5 position affected the compatibility, leading to the observed lower PV cell performance. Furthermore, *N*-substituents regardless of long or short alkyl groups did not adversely affect the PV cell performance. Our tentative theory was supported by the fact that the performance of the OPV cell fabricated from compound **8** was improved to a PCE value of 0.22% when no long alkyl groups were attached to the pyrrolidine *C*-5 position and a 3-dodecylphenyl group was present at the *C*-2 position. Unfortunately, compounds **9** and **10**, which contain different alkyl groups at the *N*-1 position of their pyrrolidine rings, showed poor device performances. These poor performance levels are attributed to their poor solubility in chloroform and the other solvents usable for the fabrication at room temperature, making it difficult to form a dense and uniform film. It is worthy to note that compound **3** containing long alkyl

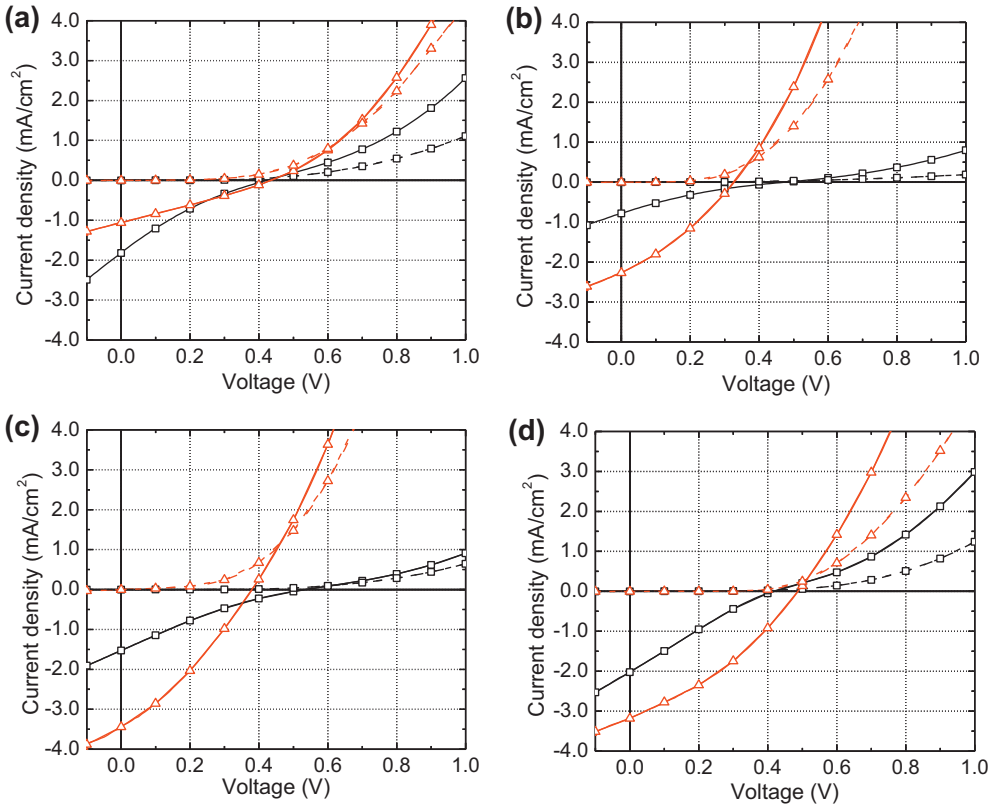

Fig. 3. *J–V* curve of the OPV cells based on the blend of P3HT and the fullerene derivatives: (a) compound **3**, (b) compound **5**, (c) compound **6**, and (d) compound **7** [dark current density, dotted line; photo current density, solid line; triangle and square indicate the mixture ratios at 2:1 and 1:1 (D:A), respectively].

group at the *N*-1 position, achieved a higher level of compatibility with P3HT than compound **1**, which did not form a homogeneous film because of the strong oil- and water-shedding properties of its C_8-perflluoroalkyl group. The coexistence of a long aliphatic alkyl group with a long fluoroalkyl group appeared to effectively relieve the oil- and water-shedding properties derived from the fluoroalkyl chain interactions.

The fullerene derivatives, **5**, **6**, and **7**, which contain short fluoroalkyl (C_6F_{13} and C_4F_9) groups, showed better performance levels in a series of fluoroalkyl fullerene derivatives because of their good compatibility with P3HT in the film blend. The highest performance in this series was achieved by the OPV cell fabricated from compound **7**, which contains a C_4F_9 group, with a V_{oc} of 0.49 V, J_{sc} of 3.18 mA/cm^2, and FF of 0.34, resulting in a PCE value of 0.53%. Compound **6** containing a C_4F_9 group also provided similar performance data, with a V_{oc} of 0.38 V, J_{sc} of 3.40 mA/cm^2, and FF of 0.41, resulting in a PCE level of 0.41%. These devices clearly demonstrate the contribution of the short fluoroalkyl-substituted fullerenes to the photocurrent generation. The effects of the fluoroalkyl and non-fluoroalkyl chain structures of the fullerene derivatives on the photovoltaic properties were consistent and reproducible. We believe that the better performances observed from the C_4-perfluoroalkyl fullerene derivatives result from the tuned nature of the aggregation of the fluoroalkyl groups, which leads to better compatibility with the donor polymer and results in a more effective BHJ structure in the blend film. On the basis of this assertion and the general findings of the current study, there is obviously a need for compromise between the intermolecular interactions of the fluoroalkyl groups and their compatibility with the donor polymer during the design of novel fluoroalkyl fullerene derivatives for use in OPV cells.

Table 2
Output parameters of the OPV cells based on blend films of P3HT and the fullerene derivative.

Compound	P3HT:fullerene (w/w)	J_{sc} (mA/cm^2)	V_{oc} (V)	FF	PCE (%)
1	2:1	1.17	0.46	0.26	0.14
2	1:1	0.90	0.41	0.16	0.06
3	1:1	1.82	0.42	0.19	0.14
4	1:1	0.88	0.42	0.22	0.08
5	2:1	2.27	0.33	0.31	0.23
6	2:1	3.40	0.38	0.41	0.41
7	2:1	3.18	0.49	0.34	0.53
8	2:1	2.86	0.31	0.24	0.22
9	1:1	1.23	0.27	0.25	0.08
10	2:1	0.40	0.20	0.24	0.02
$PC_{61}BM$	1:0.7	7.40	0.59	0.50	2.18

3.5. Surface morphology and film crystallinity

The morphology and crystallinity of the photoactive-layer are important factors in determining the overall performance of BHJ OPV cells [1–3]. With this in mind, atomic force microscopy (AFM) and X-ray diffraction measurements were conducted to assess these properties in our own materials.

A comparison of the AFM images for the C_8- and C_4-perfluoroalkyl fullerene derivatives is shown in Fig. 4, clearly showing the smooth and flat surface images of the films, which were confirmed by the fact that the surface root-mean-square roughness of the P3HT blend films with compounds **3**, **4**, **6**, and **7** were 0.72, 1.34, 1.26, and 0.93 nm, respectively. There was, however, an obvious difference in the blend films. Fig. 4c and d shows a nano-order grain-like topography of the **6** and **7** blends, respectively, which indicates the potential aggregation of the C_4-perfluoroalkyl fullerene derivatives confined within the P3HT matrix. The nano-grains observed here may have contributed to

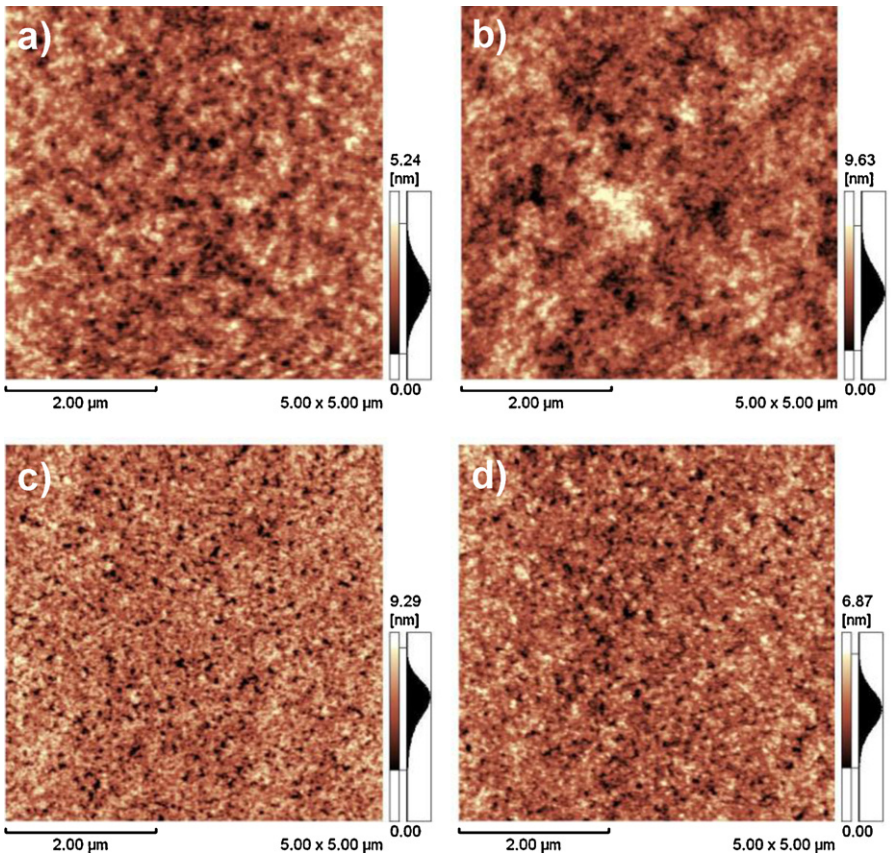

Fig. 4. AFM images of the blend films for OPV cells using the fullerene derivatives: (a) compound **3**, (b) compound **4**, (c) compound **6**, and (d) compound **7**.

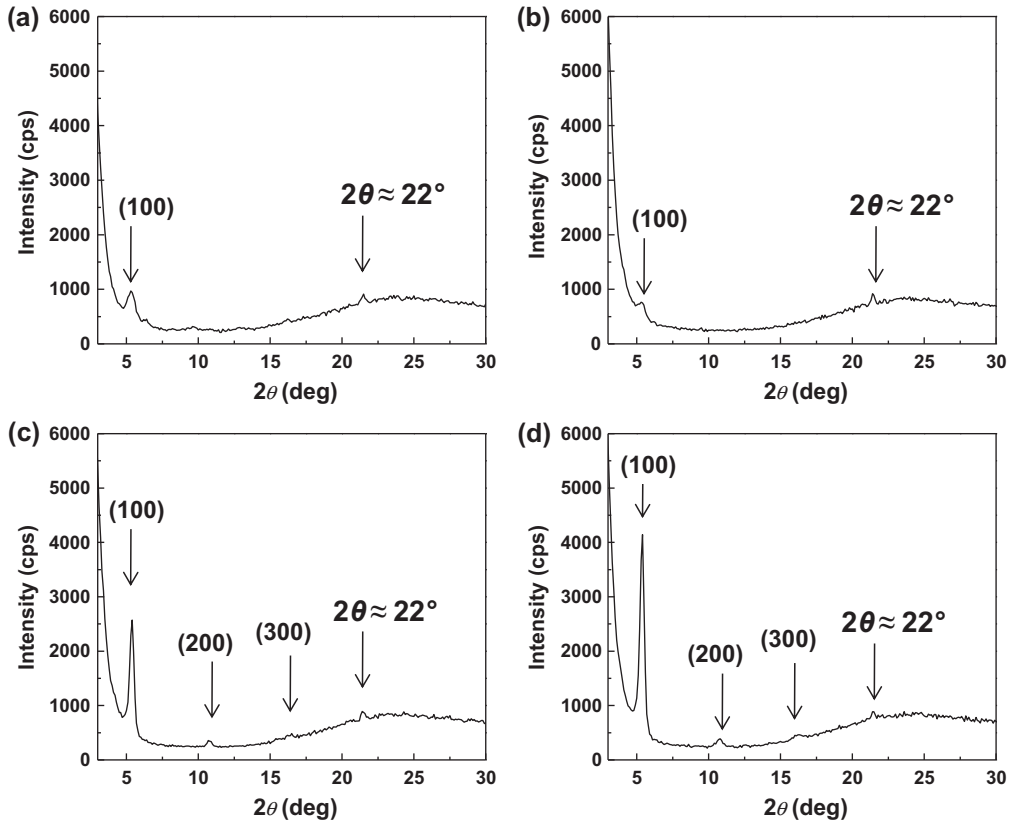

Fig. 5. X-ray diffractograms of the blend films for OPV cells using the fullerene derivatives: (a) compound **3**, (b) compound **4**, (c) compound **6**, and (d) compound **7**.

the better photovoltaic performance observed in the C_4-perfluoroalkyl fullerene derivatives relative to the C_8-perfluoroalkyl fullerene derivatives **3** and **4** (Fig. 4a and b) and the other fluoro and non-fluoroalkyl fullerene derivatives (AFM images not shown).

The X-ray diffraction results revealed clear differences in the crystallinity of the blend films (Fig. 5), with the results resembling the trend observed in the corresponding AFM images (Fig. 4). In Fig. 5a and b, the peak at $2\theta \approx 5^\circ$ corresponds to the crystallographic direction along the alkyl side chain (1 0 0) of P3HT [33]. The peak at $2\theta \approx 22^\circ$ arises from the ITO electrode [1]. In Fig. 5c and d, both of the high order ((2 0 0) and (3 0 0)) and intense (1 0 0) peaks were observed, suggesting that the structures of the films fabricated from the C_4-perfluoroalkyl fullerene derivatives were highly crystalline. Differences in the morphology and crystallinity of the films have a decisive influence on the formation of an efficient charge generation interface in the OPV cells [8].

4. Conclusion

Novel [60]fullerene derivatives bearing a fluoroalkyl group were synthesized, and their absorbance, electrochemical, and photovoltaic properties were investigated. All of the fullerene derivatives exhibited absorption ranges and reduction potential values similar to those of $PC_{61}BM$. The substituents on the pyrrolidine ring did not affect the frontier-orbital energy levels of the corresponding fullerene derivatives. The BHJ OPV cells were fabricated with an ITO/PEDOT-PSS/P3HT:fullerene derivative/Al configuration and examined under simulated AM 1.5 G solar irradiation. The fullerene derivatives with a short fluoroalkyl (C_4F_9) group gave a better level of performance than the other fluoroalkyl fullerene derivatives, and clearly demonstrated the contribution of the short fluoroalkyl fullerene derivative to the generation of the photocurrent. Taken together, these results suggest the requirement for a compromise between the intermolecular interactions of the fluoroalkyl groups and the compatibility of these with the donor polymer during the design and synthesis of novel fluoroalkyl fullerene derivatives for use in OPV cells.

These results represent so far the first report of the successful use of fluoroalkyl fullerene derivatives as the acceptor material in a polymer solar cell. As part of our ongoing research, we plan to focus on the structural optimization of the fullerene derivatives to further improve the morphology related to the PCE in the blend film. Optimization work will involve changing the substituent groups of the fullerene and replacing P3HT with other polymers to effectively tune the compatibility of the polymer with the fluoroalkyl fullerene derivatives.

Acknowledgements

This work was supported through a cooperative research program with Daikin Co., Ltd. We would like to extend our thanks to the Comprehensive Analysis Center at the Institute for Scientific and Industrial Research of Osaka University for their assistance with the elemental analyses and NMR spectroscopic measurements.

Appendix A. Supplementary data

Supplementary data associated with this article can be found, in the online version, at http://dx.doi.org/10.1016/j.jfluchem.2012.09.009.

References

[1] W. Ma, C. Yang, X. Gong, K. Lee, A.J. Heeger, Advanced Functional Materials 15 (2005) 1617–1622.
[2] G. Li, V. Shrotriya, J. Huang, Y. Yao, T. Moriarty, K. Emery, Y. Yang, Nature Materials 4 (2005) 864–868.
[3] K. Kim, J. Liu, M.M.A.G. Namboothiry, D.L. Carroll, Applied Physics Letters 90 (2007) 163511.
[4] H. Tang, G. Lu, L. Li, J. Li, Y. Wang, X. Yang, Journal of Materials Chemistry 20 (2010) 683–688.
[5] M.T. Dang, L. Hirsch, G. Wantz, Advanced Materials 23 (2011) 3597–3602.
[6] C.N. Hoth, S.A. Choulis, P. Schilinsky, C.J. Brabec, Advanced Materials 19 (2007) 3973–3978.
[7] S.-S. Kim, S.-I. Na, J. Jo, G. Tae, D.-Y. Kim, Advanced Materials 19 (2007) 4410–4415.
[8] J.W. Jung, W.H. Jo, Advanced Functional Materials 20 (2010) 2355–2363.
[9] Y.-J. Cheng, S.-H. Yang, C.-S. Hsu, Chemical Reviews 109 (2009) 5868–5923.
[10] G. Dennler, M.C. Scharber, C.J. Brabec, Advanced Materials 21 (2009) 1323–1338.
[11] P.-L.T. Boudreault, A. Najari, M. Leclerc, Chemistry of Materials 23 (2011) 456–469.
[12] H.J. Son, F. He, B. Carsten, L. Yu, Journal of Materials Chemistry 21 (2011) 18934–18945.
[13] A. Facchetti, Chemistry of Materials 23 (2011) 733–758.
[14] H. Zhou, L. Yang, W. You, Macromolecules 45 (2012) 607–632.
[15] L. Zheng, Q. Zhou, X. Deng, M. Yuan, G. Yu, Y. Cao, Journal of Physical Chemistry B 108 (2004) 11921–11926.
[16] M. Lenes, G.-J.A.H. Wetzelaer, F.B. Kooistra, S.C. Veenstra, J.C. Hummelen, P.W. Blom, Advanced Materials 20 (2008) 2116–2119.
[17] S.H. Park, C. Yang, S. Cowan, J.K. Lee, F. Wudl, K. Lee, A.J. Heeger, Journal of Materials Chemistry 19 (2009) 5624–5628.
[18] C. Yang, J.Y. Kim, S. Cho, J.K. Lee, A.J. Heeger, F. Wudl, Journal of the American Chemical Society 130 (2008) 6444–6450.
[19] P.A. Troshin, H. Hoppe, J. Renz, M. Egginger, J.Y. Mayorova, A.E. Goryachev, A.S. Peregudov, R.N. Lyubovskaya, G. Gobsch, N.S. Sariciftci, V.F. Razumov, Advanced Materials 19 (2009) 779–788.
[20] P.A. Troshin, E.A. Khakina, M. Egginger, A.E. Goryachev, S.I. Troyanov, A. Fuchsbauer, A.S. Peregudov, R.N. Lyubovskaya, V.F. Razumov, N.S. Sariciftci, ChemSusChem 3 (2010) 356–366.
[21] G. Zhao, Y. He, Z. Xu, J. Hou, M. Zhang, J. Min, H.-Y. Chen, M. Ye, Z. Hong, Y. Yang, Y. Li, Advanced Functional Materials 20 (2010) 1480–1487.
[22] M. Chikamatsu, A. Itakura, Y. Yoshida, R. Azumi, K. Yase, Chemistry of Materials 20 (2008) 7365–7367.
[23] Y. Horii, K. Sakaguchi, M. Chikamatsu, R. Azumi, K. Yase, M. Kitagawa, H. Konishi, Applied Physics Express 3 (2010) 101601.
[24] Q. Wei, T. Nishizawa, K. Tajima, K. Hashimoto, Advanced Materials 20 (2008) 2211–2216.
[25] J. Li, H. Grennberg, Chemistry: A European Journal 12 (2006) 3869–3875.
[26] E. Olmo, A. Plaza, A. Muro, A.R. Martinez-Fernandez, J.J. Nogal-Ruiz, J.L. Lopez-Perez, A.S. Feliciano, Bioorganic and Medicinal Chemistry Letters 16 (2006) 6091–6095.
[27] M.J. O'Donnell, W.A. Bruder, B.W. Daugherty, D. Liu, K. Wojciechowski, Tetrahedron Letters 25 (1984) 3651–3654.
[28] K.J.L. Paciorek, S.R. Masuda, J.G. Shih, J.H. Nakahara, Journal of Fluorine Chemistry 53 (1991) 233–248.
[29] P. Wang, B. Chen, R.M. Metzger, T. Da Ros, M. Prato, Journal of Materials Chemistry 7 (1997) 2397–2400.
[30] M. Maggini, G. Scorrano, M. Prato, Journal of the American Chemical Society 115 (1993) 9798–9799.
[31] Y. Ie, K. Nishida, M. Karakawa, H. Tada, Y. Aso, Journal of Organic Chemistry 76 (2011) 6604–6610.
[32] Unpublished data, $\mu_e \approx 10^{-2}$–10^{-3} cm^2/V s.
[33] M. Karakawa, M. Chikamatsu, Y. Yoshida, M. Oishi, R. Azumi, K. Yase, Applied Physics Express 1 (2008) 061802.